Rotation-tunneling spectrum of the deuterated ammonia dimer

E. N. Karyakin
Molecular Spectroscopy Laboratory, Applied Physics Institute, Nizhnii Novogorod, Russia

G. T. Fraser
Optical Technology Division, National Institute of Standards and Technology, Gaithersburg, Maryland 20899

J. G. Loeser and R. J. Saykally
Department of Chemistry, University of California, Berkeley, California 94720

(Received 23 November 1998, accepted 22 February 1999)

The millimeter and submillimeter-wave molecular-beam spectrum of the perdeuterated ammonia dimer $(ND_3)_2$ has been measured between approximately 50 and 400 GHz using an electric-resonance optothermal spectrometer (EROS). As in the case of the $(NH_3)_2$, the spectrum is complicated by the threefold internal rotation of the ND_3 subunits, the interchange tunneling of the two subunits, and the inversion of the subunits through their respective centers of masses. These tunneling motions split the rigid-molecule energy levels into 22 components, which all have nonzero statistical weights in the case of the deuterated dimer. Transitions have been assigned for rotation-tunneling states correlating to $A-A$ (*ortho–ortho*) combinations of the ND_3 monomer states, where A designates the rovibronic symmetries of the ND_3 subunits. One $K=1\leftarrow 1$, one $K=1\leftarrow 0$, one $K=0\leftarrow 1$, and two $K=0\leftarrow 0$ progressions have been assigned. The data have been fit to 0.28 MHz using linear molecule-type energy-level expressions to determine rotational constants, band origins, ℓ/K-type double constants, and centrifugal distortion constants. The two $K=0\leftarrow 0$ subbands, with origins near 264 GHz, are split by 64 MHz due to monomer inversion, as observed previously in the NH_3 dimer. The 264 GHz, $K=0$ splitting arises predominantly from monomer interchange tunneling and is nearly a factor of 2 less than the 483 GHz value for the NH_3 dimer. The separation is also approximately 25% smaller than predicted by Olthof *et al.* [E. H. T. Olthof, A. van der Avoird, and P. E. S. Wormer, J. Chem. Phys. **101**, 8430 (1994)] from dynamical calculations on a model potential energy surface adjusted to fit the observed far-infrared rotation-tunneling spectrum of the NH_3 dimer. © *1999 American Institute of Physics.* [S0021-9606(99)01419-1]

I. INTRODUCTION

An understanding of the structure and dynamics of the ammonia dimer has been of great interest since Nelson *et al.*[1,2] concluded from an analysis of the microwave spectrum of the dimer that it has a rigid nonhydrogen-bonded geometry, in disagreement with a number of high-level *ab initio* calculations.[3] Their arguments were based on the observation of a series of $K=0$ rigid-rotor transitions of several isotopic forms of the dimer. For the totally protonated dimers, the $K=0$ transitions are split by less than 1 MHz, with the splitting attributed to internal rotation of one of the monomer subunits about its threefold axis. The *a*-inertial-axis components of the electric dipole moment and ^{14}N quadrupole coupling constants were found to be only weakly sensitive to isotopic substitution, which led to the conclusion that the complex is rigid since these quantities arise primarily from zero-point projections of the monomer values. The absence of donor–acceptor interchange was particularly puzzling since such effects were observed previously in a number of homogenous dimers, such as $(HF)_2$ and $(H_2O)_2$.

In a follow-up study, Nelson and Klemperer[4] addressed this problem using a group theoretical analysis based on the G_{36} molecular symmetry group, valid for an NH_3 dimer in which monomer inversion is quenched. They concluded that the observed states in the microwave spectrum consist of mixed combinations of A and E symmetry monomer states. For these states, the interchange tunneling will be quenched if the internal rotation effects are large compared to the interchange tunneling matrix elements.

A subsequent analysis by Loeser *et al.*[5] of the far-infrared spectrum of the NH_3 dimer[5–7] revealed that the spectrum of the dimer is significantly more complex than initially suggested by the microwave study. Loeser *et al.*[5] found, in fact, that the monomer inversion motion is not quenched in the dimer, thus requiring the use of the G_{144} molecular symmetry group in the analysis. Havenith *et al.*[7] came to similar conclusions from an infrared–far-infrared double-resonance study of the dimer.

The detailed far-infrared analysis of Loeser *et al.*[5] motivated a quantum mechanical calculation of the rotation-tunneling states of the NH_3 dimer on an adjustable model potential by Olthof *et al.*,[8] using a methodology developed previously.[9,10] Their calculations suggest an equilibrium configuration significantly distorted from a linear hydrogen-bonded minimum with an extremely low barrier ($\sim 7\ cm^{-1}$) for the tunneling interchange of the bonding roles of the two monomers. Predictions from the model potential[8,11] agree well with the microwave, far-infrared, and infrared spectrum[1,2,5–7,12] and with electric dipole moments[1,2,13,14] and nuclear quadrupole coupling constant values[1,2,15] avail-

able prior to and after the this work, with the exception of the measured asymmetry in the quadrupole coupling constant tensor $(eQq_{bb}-eQq_{cc})$, which suggests that the potential is too soft in the dihedral angle.[15] The shallowness of their potential surface is also in agreement with recent *ab initio* calculations.[16,17] The C_s-symmetry minimum suggested by Olthof *et al.*[8] contrasts with the conclusion of Tao and Klemperer,[17] who conclude from their calculations (6-311 $+G(3d,2p)$ and $[7s5p3d,4s1p]$ extended with bond functions) that the minimum-energy configuration has C_{2h} symmetry.

Olthof *et al.*[8] also gave predictions for the tunneling splittings in the ND_3 dimer. Measurements of these splittings, which are presented here, furnish an additional critical test of the model potential energy surface of Olthof *et al.*[8] In addition, because of its reduced zero-point energy, the ND_3 dimer spectrum should be more sensitive to the shape of the equilibrium configuration of the dimer. Thus, ND_3 dimer data, when combined with the appropriate theoretical analysis, may be useful for discriminating between the Olthof *et al.*[8] C_s minimum and the Tao and Klemperer[17] C_{2h} minimum.

In the present work, we present measurements of the rotation-tunneling spectrum of ND_3 dimer states correlating asymptotically to *A*-symmetry monomer rovibronic states. Measurements were made for both $K=0$ and $K=1$. The spectra are complicated by $K=0/K=1$ Coriolis interactions and by monomer inversion. These effects have been previously observed in the NH_3 dimer, and help verify the present assignments. The observed $K=0$ interchange splitting is approximately 25% smaller than the predicted value of Olthof *et al.*,[8] suggesting the need for refinement of their potential.

II. EXPERIMENT

The present measurements were made using an electric-resonance optothermal spectrometer (EROS), as described previously.[18–20] Briefly, a molecular beam of ND_3 dimer is produced by a supersonic expansion of several percent ND_3 seeded in argon through a 40 μm diameter nozzle at a backing pressure of 250 to 300 kPa. The molecular beam is defined by a 1-mm diameter skimmer located approximately 2.5 cm from the nozzle. After leaving the skimmer, the beam travels through a 56-cm-long electrostatic field of quadrupolar symmetry and then strikes a 1.7 K liquid-He-cooled bolometer detector. The electrostatic field focuses molecules in rotation-tunneling states with positive Stark coefficients (states whose energies increase with field strength) onto the bolometer detector. Molecules in states with negative Stark coefficients are deflected out of the molecular bcam. Millimeter and submillimeter radiation is applied to the molecular beam between the nozzle and skimmer using a cutoff section of *K*-band waveguide. The radiation is furnished by phase-locked backward-wave oscillators (BWO).[21] A resonance is observed when the beam intensity at the bolometer is changed due to the different focusing behavior of the upper and lower states of the transition in the quadrupole field. In practice, the radiation is either frequency or amplitude modulated and the bolometer output is monitored as a function of BWO frequency with a phase-sensitive detector. A sample spectrum is shown in Fig. 1.

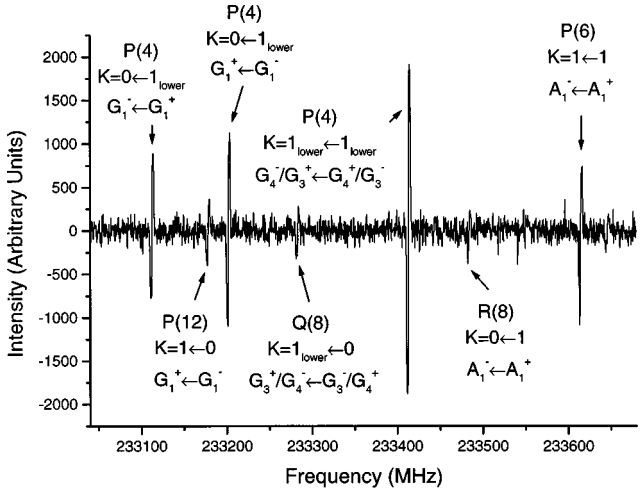

FIG. 1. Sample millimeter wave spectrum of $(ND_3)_2$ near 233.4 GHz. The assignments of the transitions are given. The spectrum required approximately 6 min to acquire.

III. RESULTS

Approximately 650 transitions have been observed in the He/ND_3 expansion, 106 of which have been assigned to ND_3 dimers states correlating to free monomer states of *A* rovibronic symmetry (i.e., designated $A-A$). The assigned transitions are listed in Table I and an energy-level diagram for the $A-A$ states with nuclear-spin statistical weight factors[11] is shown in Fig. 2. As seen in Fig. 2, the $K=0$ and $K=1$ states are each split into doublets (264 GHz for $K=0$ and 286 GHz for $K=1$), due primarily to the interchange tunneling. These states have rotation-tunneling symmetries of A_1, A_2, A_3, and A_4 in the G_{36} molecular symmetry group. Coriolis interactions, predominantly between the observed $K=0$ and $K=1$ states, split each $K=1$ level into a doublet, analogous to *K*-type or ℓ-type doubling. The $K=0$ and ℓ/K-doubled $K=1$ states are further split into three components $(A_1^+/E^-/B_2^+,\ A_1^-/E^+/B_2^-,\ B_1^+/E^-/A_2^+,$ or $B_1^-/E^+/A_2^-)$ due to monomer inversion. When monomer inversion is resolved, as in the present study, the states are labeled using the G_{144} molecular symmetry group, as discussed by Loeser *et al.*[5] In G_{144}, the selection rules are $A_1^+\leftrightarrow A_1^-$, $A_2^+\leftrightarrow A_2^-$, $B_1^+\leftrightarrow B_1^-$, $B_2^+\leftrightarrow B_2^-$, and $E^+\leftrightarrow E^-$.

One $K=1\leftarrow 1$, one $K=1\leftarrow 0$, one $K=0\leftarrow 1$, and two $K=1\leftarrow 0$ progressions have been assigned. The two $K=0\leftarrow 0$ bands, with origins separated by ~64 MHz, are assigned to the $A_1^\pm/B_1^\pm$ and $E^\pm$ components of the monomer-inversion-split $K=0\leftarrow 0$ band shown in Fig. 2. The $A_2^\pm/B_2^\pm$ component is not observed at the present signal-to-noise ratio due to its low statistical weight factors, which are down by approximately 2 orders of magnitude from the dominant $A_1^\pm/B_1^\pm$ component. We note that the observed relative intensities of the $A_1^\pm/B_1^\pm$ and $E^\pm$ subbands and the similarity of the rotational constants for the two bands are consistent with this assignment. For the other bands, only the strong $A_1^\pm/B_1^\pm$

TABLE I. Observed transition frequencies (in MHz)[a] for the $A-A$ (*ortho-ortho*) states of $(ND_3)_2$.

J'	Sym.′	K'/l'	J''	Sym.″	K''/l''	Frequency	J'	Sym.′	K'/l'	J''	Sym.″	K''/l''	Frequency
9	A_1^-	0	10	A_1^+	0	174 344.8	7	A_1^-	0	6	A_1^+	1	219 279.9
7	A_1^-	0	8	A_1^+	0	193 342.3	9	A_1^-	0	8	A_1^+	1	233 484.2
6	B_1^+	0	7	B_1^-	0	202 659.2	10	B_1^+	0	9	B_1^-	1	240 350.8
5	A_1^-	0	6	A_1^+	0	211 851.3	11	A_1^-	0	10	A_1^+	1	247 060.7
4	B_1^+	0	5	B_1^-	0	220 918.1	12	B_1^+	0	11	B_1^-	1	253 615.0
3	A_1^-	0	4	A_1^+	0	229 856.6	13	A_1^-	0	12	A_1^+	1	260 014.4
2	B_1^+	0	3	B_1^-	0	238 665.9	7	A_1^-	1	8	A_1^+	0	315 643.7
1	A_1^-	0	2	A_1^+	0	247 344.6	6	B_1^+	1	7	B_1^-	0	324 748.6
0	B_1^+	0	1	B_1^-	0	255 891.4	5	A_1^-	1	6	A_1^+	0	333 760.0
1	A_1^-	0	0	A_1^+	0	272 584.8	4	B_1^+	1	5	B_1^-	0	342 675.3
2	B_1^+	0	1	B_1^-	0	280 730.5	3	A_1^-	1	4	A_1^+	0	351 493.1
3	A_1^-	0	2	A_1^+	0	288 741.0	2	B_1^+	1	3	B_1^-	0	360 211.6
4	B_1^+	0	3	B_1^-	0	296 615.6	8	B_1^+	1	9	B_1^-	1	205 781.7
5	A_1^-	0	4	A_1^+	0	304 354.5	7	A_1^-	1	8	A_1^+	1	215 174.1
6	B_1^+	0	5	B_1^-	0	311 957.7	6	B_1^+	1	7	B_1^-	1	224 452.4
7	A_1^-	0	6	A_1^+	0	319 425.2	5	A_1^-	1	6	A_1^+	1	233 614.7
8	B_1^+	0	7	B_1^-	0	326 756.7	4	B_1^+	1	5	B_1^-	1	242 658.9
9	A_1^-	0	8	A_1^+	0	333 953.8	3	A_1^-	1	4	A_1^+	1	251 584.0
10	B_1^+	0	9	B_1^-	0	341 016.0	2	B_1^+	1	3	B_1^-	1	260 387.8
11	A_1^-	0	10	A_1^+	0	347 943.8	2	A_1^-	−1	2	A_1^+	1	285 514.4
12	B_1^+	0	11	B_1^-	0	354 739.2	3	B_1^+	−1	3	B_1^-	1	284 963.8
13	A_1^-	0	12	A_1^+	0	361 401.6	4	A_1^-	−1	4	A_1^+	1	284 230.8
6	E^-	0	7	E^+	0	202 722.0	5	B_1^+	−1	5	B_1^-	1	283 315.1
5	E^+	0	6	E^-	0	211 914.7	6	A_1^-	−1	6	A_1^+	1	282 218.3
4	E^-	0	5	E^+	0	220 983.1	2	B_1^+	1	1	B_1^-	1	302 559.8
3	E^+	0	4	E^-	0	229 920.2	4	B_1^+	1	3	B_1^-	1	318 549.7
2	E^-	0	3	E^+	0	238 729.6	5	A_1^-	1	4	A_1^+	1	326 354.0
1	E^+	0	2	E^-	0	247 408.3	6	B_1^+	1	5	B_1^-	1	334 031.0
0	E^-	0	1	E^+	0	255 954.9	7	A_1^-	1	6	A_1^+	1	341 581.0
1	E^+	0	0	E^-	0	272 649.0	8	B_1^+	1	7	B_1^-	1	349 003.3
2	E^-	0	1	E^+	0	280 794.0	9	A_1^-	1	8	A_1^+	1	356 299.5
3	E^+	0	2	E^-	0	288 804.7	10	B_1^+	1	9	B_1^-	1	363 468.0
4	E^-	0	3	E^+	0	296 679.3	9	B_1^+	−1	10	B_1^-	−1	196 206.3
5	E^+	0	4	E^-	0	304 418.2	8	A_1^-	−1	9	A_1^+	−1	205 768.2
6	E^-	0	5	E^+	0	312 021.5	7	B_1^+	−1	8	B_1^-	1	215 207.7
7	E^+	0	6	E^-	0	319 488.8	6	A_1^-	−1	7	A_1^+	−1	224 522.3
9	E^+	0	8	E^-	0	334 017.7	5	B_1^+	−1	6	B_1^-	−1	233 709.8
10	E^-	0	9	E^+	0	341 079.5	4	A_1^-	−1	5	A_1^+	−1	242 768.3
13	E^+	0	12	E^-	0	361 464.3	3	B_1^+	−1	4	B_1^-	−1	251 695.4
1	A_1^-	0	1	A_1^+	−1	164 501.6	2	A_1^-	−1	3	A_1^+	−1	260 490.2
2	B_1^+	0	2	B_1^-	−1	164 283.9	2	B_1^+	1	2	B_1^-	−1	285 829.3
3	A_1^-	0	3	A_1^+	−1	163 957.9	3	A_1^-	1	3	A_1^+	−1	285 594.7
4	B_1^+	0	4	B_1^-	−1	163 524.7	4	B_1^+	1	4	B_1^-	−1	285 281.9
5	A_1^-	0	5	A_1^+	−1	162 983.4	5	A_1^-	1	5	A_1^+	−1	284 891.5
6	B_1^+	0	6	B_1^-	−1	162 335.6	2	A_1^-	−1	1	A_1^+	−1	302 430.2
7	A_1^-	0	7	A_1^+	−1	161 583.1	3	B_1^+	−1	2	B_1^-	−1	310 405.0
9	A_1^-	0	9	A_1^+	−1	159 765.5	4	A_1^-	−1	3	A_1^+	−1	318 241.9
10	B_1^+	0	10	B_1^-	−1	158 703.7	5	B_1^+	−1	4	B_1^-	−1	325 937.9
2	B_1^+	0	1	B_1^-	1	181 014.0	6	A_1^-	−1	5	A_1^+	−1	333 496.3
3	A_1^-	0	2	A_1^+	1	188 981.9	7	B_1^+	−1	6	B_1^-	−1	340 915.5
4	B_1^+	0	3	B_1^-	1	196 792.7	8	A_1^-	−1	7	A_1^+	−1	348 196.6
5	A_1^-	0	4	A_1^+	1	204 445.7	9	B_1^+	−1	8	B_1^-	−1	355 340.7
6	B_1^+	0	5	B_1^-	1	211 941.8	10	A_1^-	−1	9	A_1^+	−1	362 347.3

[a]The uncertainties on the line positions are 0.25 MHz (type A standard uncertainties).

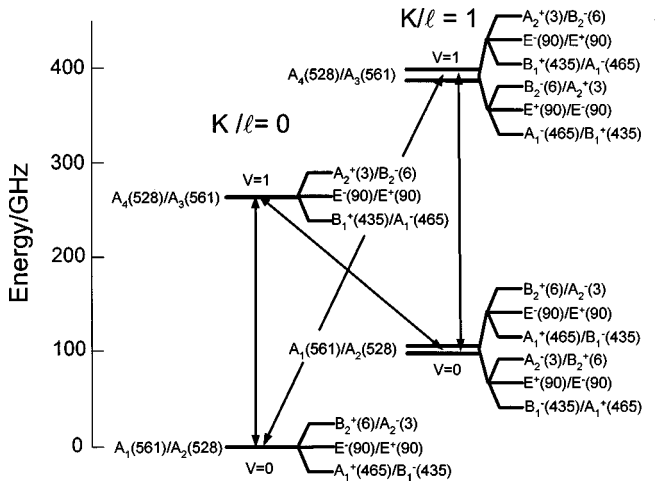

FIG. 2. Energy-level diagram of the $(ND_3)_2$ showing states which correlate asymptotically to A rovibronic symmetry monomer units. The $G_{36}(A_1,A_2,A_3,A_4)$ and G_{144} rotation-tunneling symmetries are shown together with the nuclear-spin statistical weights (Ref. 11) in parentheses. For $K=0$, the levels are split into three components due to ND_3 monomer inversion. For $K=1$, the levels are shown first splitting into two components by Coriolis interaction with $K=0$ and then split into three components from ND_3 monomer inversion. The Coriolis and monomer inversion splittings are greatly exaggerated in the figure. The arrows designate the observed transitions.

component was assigned, due to the lower signal-to-noise ratio for these bands arising from the reduced thermal population of their lower-state progenitors.

The observed transitions have been least-squares fit to the linear-molecular-like energy-level expression,

$$E(v,J,K,\pm)=E_v+B_v[J(J+1)-K^2] - D_v[J(J+1)-K^2]^2\pm q_v\delta_{K,1}J(J+1) \pm d_v\delta_{K,1}[J(J+1)]^2,$$

where B is a rotation constant, D is a centrifugal distortion constant, q is an ℓ-doubling constant, and v is a state label, as given in Fig. 2. For an asymmetric rotor $q_v\equiv(B_v-C_v)/4$, while for a linear molecular, $q_v\equiv q_\ell/2$, where q_ℓ is the standard ℓ-doubling constant. The q_v were constrained to be positive by using the + factor in front of q_v and d_v for the upper energy components of the K/ℓ doublets. All the transitions were weighted equally in the fit. The spectroscopic constants resulting from the fit with their type A standard uncertainties are given in Table II. The standard deviation of the fit is 0.28 MHz, and is close to our typical measurement reproducibility of 0.25 MHz and nearly a factor of 10 smaller than the 2 to 2.5 MHz FWHM linewidths of the transitions.

The spectroscopic constants in Table II show several interesting features. First, we see that the B and D values for the $v=0$ states for $K=0$ and 1 are nearly identical, and similarly for $v=1$. The rotational constant for the $v=0$ state is also close to the value of 4190.3 MHz[1] determined for the $\ell/K=0$, $v=0$ state of the $A-E$ (*ortho–para*) $(ND_3)_2$ state. These observations suggest that the 1.6% change in rotational constants between the $v=0$ and 1 states is a consequence of the different zero-point radial separations of the symmetric and antisymmetric interchange tunneling states. A 1.6% difference in rotational constants corresponds to an $\sim$3.2% difference in $\langle 1/r^2\rangle^{-1/2}$ values between the two states (i.e., $\sim$0.11 Å), where r is the center-of-mass separation and the averaging is over the zero-point motion. The bond length for $(ND_3)_2$ has been previously shown to be $\langle 1/r^2\rangle^{-1/2}=3.35$ Å.[1]

The signs of the ℓ/K-type doublet splittings are consistent with the splittings originating from Coriolis interactions between the $K=1$ and $K=0$ states through a matrix element with $\Delta v=0$. The magnitude of these matrix elements can be estimated if we assume that the ℓ/K-type splitting arises solely from Coriolis interactions with the $K=0$ state of the same v. For the $J=1$, $v=0$, $K=1$ state, a coupling matrix element of $\Delta_{0,1}(J=1)=2150$ MHz to the $J=1$, $v=0$, $K=0$ state accounts for the observed 46.4 MHz splitting of the $J=1$, $v=0$, $K=1$ state. The 58.7 MHz splitting of the $J=1$, $v=1$, $K=1$ state is accounted for by a matrix element of $\Delta_{0,1}(J=1)=2670$ MHz to the $J=1$, $v=1$, $K=0$ state. In the case of unquenched ''vibrational'' angular momentum, $\Delta_{0,1}(J)=2B[J(J+1)]^{1/2}$, which equals $\sim$11 900 MHz for $J=1$.

IV. DISCUSSION

The measured interchange splittings in the present study can be compared with values calculated by Olthof *et al.*[8] on a potential-energy surface optimized primarily to characterize the microwave and far-infrared spectrum of the NH_3 dimer. They predict a $K=0$, $A-A$ interchange tunneling splitting of 331 GHz, compared to our observed value of 264 GHz. We note that in the $(NH_3)_2$, the experimental interchange splitting is 483 GHz, while the potential modeling gives an $(NH_3)_2$ splitting of 475 GHz. The experimental ratio for the $(NH_3)_2/(ND_3)_2$ $K=0$ splitting of 1.83 is closer to the free-rotor value of 2, than the harmonic value of $2^{1/2}$.

TABLE II. Spectroscopic constants (in MHz)[a] for the $A-A$ (*ortho–ortho*) states of $(ND_3)_2$.

	$v=0, A_1^{\pm}/B_1^{\pm}$	$v=1, A_1^{\pm}/B_1^{\pm}$	$v=0, E^{\pm}$	$v=1, E^{\pm}$	v=0, $A_1^{\pm}/B_1^{\pm}$	$v=1, A_1^{\pm}/B_1^{\pm}$
E_v	0.000	264305.06(11)	0.0	264368.81(11)	103900.90(15)	389900.57(17)
B_v	4206.9893(89)	4140.0660(73)	4206.922(20)	4140.007(18)	4206.0097(75)	4140.4275(80)
D_v	0.037115(71)	0.030434(50)	0.03600(26)	0.02965(20)	0.036564(57)	0.029734(61)
q_v	⋯	⋯	⋯	⋯	11.5900(24)	14.6871(28)
d_v	⋯	⋯	⋯	⋯	0.000518(27)	−0.000657(34)

[a]Type A standard uncertainties are given in parantheses (i.e., coverage factor $k=1$).

The ratio for the Olthof *et al.*[8] potential of 1.44 is close to the harmonic limit, as noted by these authors. Our measurements suggest that the interchange motion in the ammonia dimer more closely resembles a hindered free-rotation than suggested by the potential of Olthof *et al.*[8] Along this lines, it is noteworthy that the polar angles, their θ_i, determined from the quadrupole coupling constants of 48.6 and 64.5 deg for $(NH_3)_2$ and 49.6 and 62.6 deg $(ND_3)_2$, are close to the ''magic'' angle value of 54.7 deg for vanishing $\langle P_2(\cos\theta_i)\rangle$, which results when the averaging is taken over free-rotor large-amplitude vibrational functions.

Olthof *et al.*[11] have also calculated the monomer inversion splittings for the $K=0$ states of $(ND_3)_2$. They determine that the $A_2^+ - B_1^+$ splittings for the $v=1$, $K=0$ state is 70.6 MHz assuming that the monomer inversion splitting is unchanged upon complexation. Assuming a 9% lowering of the barrier, as indicated for the $(NH_3)_2$, gives a value of 148.3 MHz for this splitting. Likewise, for the $B_2^+ - A_1^+$ splitting for $v=0$, $K=0$ they estimated a value of 37.0 MHz for no change in barrier and a value of 77.7 MHz if the barrier is lowered by 9%. Under the assumption that the E states are midway between their A/B partners, we find that the $A-B$ tunneling splitting increases by 127.5 MHz from $v=0$ and 1. This can be compared to values of 33.6 and 70.6 MHz, calculated theoretically for no barrier change and a 9% barrier change, respectively. This disagreement between theory and experiment suggests a greater reduction of the inversion barrier upon complexation or the need for some refinements in the proposed pair potential.

We have also measured and assigned a number of transitions for rotation-tunneling states of the dimers having $A-E$ and $E-E$ monomer progenitors. At present, this assignment is incomplete and awaits further experimental measurements. Some of the assignments are shown in the spectrum of Fig. 1. Complicating these assignments is the presence of a number of lines of ND_3–ND_2H from isotopic exchange and the strong Coriolis interactions between the $K=0$ and 1 components of the dimer state. In addition, a strong perturbation is observed to abruptly occur near $J=5$ for a couple of the series, which cannot yet be explained. A future paper will address these issues. It is also hoped that the availability of the present results will motivate renewed theoretical efforts to refine the NH_3 pair potential, which, in turn, can help guide the analysis of the $A-E$ and $E-E$ spectra of the $(ND_3)_2$.

ACKNOWLEDGMENTS

R.J.S. and J.G.L. acknowledge support from the Physical Chemistry Division of the National Science Foundation. E.N.K. and G.T.F. received partial funding from the U.S. Civilian Research and Development Foundation (Award No. RC1-216). E.N.K. was also supported by the Russian Foundation (RFFI 97-02-16593).

[1] D. D. Nelson, Jr., G. T. Fraser, and W. Klemperer, J. Chem. Phys. **83**, 6201 (1985).
[2] D. D. Nelson, Jr., W. Klemperer, G. T. Fraser, F. J. Lovas, and R. D. Suenram, J. Chem. Phys. **87**, 6364 (1987).
[3] For a review, see Ref. 1.
[4] D. D. Nelson, Jr. and W. Klemperer, J. Chem. Phys. **87**, 139 (1987).
[5] J. G. Loeser, C. A. Schmuttenmaer, R. C. Cohen, M. J. Elrod, D. W. Steyert, R. J. Saykally, R. E. Bumgarner, and G. A. Blake, J. Chem. Phys. **97**, 4727 (1992).
[6] M. Havenith, R. C. Cohen, K. L. Busarow, D.-H. Gwo, Y. T. Lee, and R. J. Saykally, J. Chem. Phys. **94**, 4776 (1991).
[7] M. Havenith, H. Linnartz, E. Zwart, A. Kips, J. J. ter Meulen, and W. L. Meerts, Chem. Phys. Lett. **193**, 261-268 (1992).
[8] E. H. T. Olthof, A. van der Avoird, and P. E. S. Wormer, J. Chem. Phys. **101**, 8430 (1994).
[9] J. W. I. van Bladel, A. van der Avoird, P. E. S. Wormer, and R. J. Saykally, J. Chem. Phys. **97**, 4750 (1992).
[10] E. H. T. Olthof, A. van der Avoird, and P. E. S. Wormer, J. Mol. Struct.: THEOCHEM **307**, 201 (1994).
[11] E. H. T. Olthof, A. van der Avoird, P. E. S. Wormer, J. G. Loeser, and R. J. Saykally, J. Chem. Phys. **101**, 8443 (1994).
[12] H. Linnartz, W. L. Meerts, and M. Havenith, Chem. Phys. **193**, 327 (1995).
[13] H. Linnartz, A. Kips, W. L. Meerts, and M. Havenith, J. Chem. Phys. **99**, 2449 (1993).
[14] G. Cotti, H. Linnartz, W. L. Meerts, A. van der Avoird, and E. H. T. Olthof, J. Chem. Phys. **104**, 3898 (1996).
[15] N. Heineking, W. Stahl, E. H. T. Olthof, P. E. S. Wormer, A. van der Avoird, and M. Havenith, J. Chem. Phys. **102**, 8693 (1995).
[16] D. M. Hassett, C. J. Marsden, and B. J. Smith, Chem. Phys. Lett. **183**, 449 (1991).
[17] F.-M. Tao and W. Klemperer, J. Chem. Phys. **99**, 5976 (1993).
[18] G. T. Fraser, R. D. Suenram, L. H. Coudert, J. Chem. Phys. **90**, 6077 (1989).
[19] G. T. Fraser and A. S. Pine, J. Chem. Phys. **91**, 637 (1989).
[20] G. T. Fraser, F. J. Lovas, R. D. Suenram, E. N. Karyakin, A. Grushow, W. A. Burns, and K. R. Leopold, J. Mol. Spectrosc. **181**, 229 (1997).
[21] Yu. I. Alekshin, G. M. Altshuller, O. P. Pavlovsky, E. N. Karyakin, A. F. Krupnov, D. G. Paveliev, and A. P. Shkaev, Int. J. Infrared Millim. Waves **11**, 961 (1990).